A FAILSAFE ANALYSIS USING NASTRAN'S PIECEWISE LINEAR ANALYSIS AND A NINE NODE LINEAR CRACK ELEMENT

R. F. Wilkinson and J. W. Kelley

Lockheed-Georgia Company

SUMMARY

This paper shows how a two-dimensional crack element was implemented into NASTRAN as a user dummy element and used to study failsafe characteristics of the C5A fuselage. The element is formulated from Reissner's functional requiring that it satisfy compatability with the linear boundary displacement elements in NASTRAN. Its accuracy is demonstrated by analyzing for the stress intensity factors of two simple crack configurations for which there are classic solutions.

INTRODUCTION

A Lockheed requirement during the design of the C5A was for the pressurized fuselage structure to have the capability of sustaining a longitudinal crack in the skin. Circumferential straps are attached to the skin midway between the frames to provide this capability. Conventional methods for designing the straps and the system for attaching them to the skin are conservative and as a result dictate the use of high strength fasteners. It is now possible, due to the introduction of special crack tip singularity elements, to make a finite element analysis which eliminates much of this conservatism.

Part of the criterion for determining if a crack can be arrested is to find a configuration for which the stress intensity factor at the tip of the crack is lower than the critical stress intensity factor for the skin material. NASTRAN was considered the best analysis tool with which to analyze the various crack configurations. This was due to the ease with which a crack element can be incorporated into it as a user dummy element.

LIST OF SYMBOLS

σ Stress

ϵ Strain

μ Displacement

η Vector normal to a surface

$\overset{\eta}{T}{}^*$ Applied tractions

μ^* Applied displacements

W_c Complementary energy function

F Body forces

V Volume of an element

S_σ Surface on which $\overset{\eta}{T}{}^*$ are specified

S_μ Surface on which μ^* are specified

D Interior boundary subdividing a region into finite elements

$[S]$ Compliance matrix

G Shear modulus

v Poisson's ratio

SINGULARITY CRACK ELEMENT FORMULATION

In this section the stiffness matrix and the relationship between the nodal displacements and the stress intensity factors for a crack element are developed.

Reissner's functional, Reference 1, for a region subdivided by boundaries D into finite elements gives

$$
(1) \qquad J_R = \sum \left\{ \int_V \left[-W_c(\sigma_{LK}) - F_L \mu_L + \tfrac{1}{2} \sigma_{LK}(\mu_{L,K} + \mu_{K,L}) \right] d\dot{V} \right.
$$
$$
\left. \left(-\int_{S_\sigma} \overset{\eta}{T_L^*} \mu_L dS - \int_{S_\mu} \sigma_{LK} \eta(\mu_L - \mu_L^*) dS \right) \right\}
$$

where the summation includes all the finite elements making up the region

If the displacements of the surfaces D are assumed compatible between finite elements, then the necessary conditions for J_R to be stationary due to a variation in the functions σ_{LK}, and μ_L are the following five Euler equations:

$$
(2) \qquad \frac{\partial W_c}{\partial \sigma} = \tfrac{1}{2}(\mu_{L,K} + \mu_{K,L}) \qquad \text{in} \qquad V \qquad \text{(Hook's Law)}
$$

$$
(3) \qquad \sigma_{LK,K} + F_L = 0 \qquad \text{in} \qquad V \qquad \text{(Equilibrium Equations)}
$$

$$
(4) \qquad \sigma_{LK} \, \eta_K = \overset{\eta}{T_L^*} \qquad \text{on} \qquad S_\sigma \qquad \text{(Traction boundary condition)}
$$

$$
(5) \qquad \mu_L = \mu_L^* \qquad \text{on} \qquad S_\mu \qquad \text{(Displacement boundary condition)}
$$

$$
(6) \qquad < \sigma_{LK} \, \eta_K > = 0 \qquad \text{on} \qquad D \qquad \text{(Stress continuity between elements)}
$$

In which W_c has the property $\dfrac{\partial W_c}{\partial \sigma_{LK}} = \epsilon_{LK}$

A modified form of (1) is obtained by neglecting body forces and restricting the functions $\sigma_{\iota\kappa}$ and μ_ι to the set which satisfy (3), (4), and (5)

$$(8) \qquad J_1 = \sum \left[-\int_V W_c(\sigma_{\iota\kappa}) dV + \int_{S_\mu} \sigma_{\iota\kappa} \eta_\kappa \mu_\iota^* dS + \int_D \sigma_{\iota\kappa} \eta_\kappa \mu_\iota dS \right]$$

For this form of the functional the displacements μ_ι only appear in the boundary integrals and hence do not have to be defined in the interior of the element.

In applying J_1 to the finite element shown in Figure 1 the stresses $\sigma_{\iota\kappa}$ are approximated by finite series and the displacements μ_ι are required to vary linearly between nodal displacements $\{Q\}$. This ensures displacement compatibility with the linear boundary displacement elements already in the NASTRAN system. Expressing these approximate functions in matrix form

$$(9) \qquad \{\sigma\} = [P] \{\beta\} \qquad \text{stresses in V}$$

$$(10) \qquad \{\mu_D\} = [L_D] \{Q\} \qquad \text{displacements of the surface D}$$

$$(11) \qquad \{T_D\} = [P_D] \{\beta\} \qquad \sigma_{\iota\kappa} \eta_\kappa \qquad \text{at the surface D}$$

where $[P]$ are the assumed series of stress functions and $\{\beta\}$ are the corresponding coefficients, $[L_D]$ are linear interpolations of the nodal displacements $\{Q\}$ along the boundary D, and $[P_D]$ are the values of $[P]$ that give the stresses $\{\sigma\}$ in Equation 9 normal to the boundary D. The stresses on the boundary S_μ do not have to be defined as there are no enforced boundary displacements associated with this element.

184

Substituting (9), (10), and (11) into (8) gives the contribution of the crack element to J.

(12) $\qquad J_{1c} = -\frac{1}{2} \lfloor \beta \rfloor [KC] \{ \beta \} + \lfloor \beta \rfloor [KA] \{ Q \}$

where

(13) $\qquad [KC] = \int_V [P]^T [S][P] dV$

(14) $\qquad [KA] = \int_D [P_D][L_D] dS$

Due to the fact that the coefficients, $\{\beta\}$, are independent between elements the necessary condition for J_{1c} to be stationary is $\dfrac{\partial J_{1c}}{\partial \beta} = 0$. This yields:

(15) $\qquad \beta = [KC]^{-1}[KA]\{Q\}$

Substituting (15) into (12) and finding a stationary value of J_{1c} with respect to $\{Q\}$ give the contribution of the crack element to the total stiffness matrix

(16) $\qquad [KS] = [KA]^T [KC]^{-1}[KA]$

   Each term in the series used to approximate the stresses has to satisfy equilibrium and the stress boundary conditions. The series also has to include the known stress singularity near the tip of the crack. The form that has been assumed for this element is that which was developed from the Williams series of stress functions by Aberson and Anderson in Reference 2. The two dimensional stress distributions in polar coordinates are:

$$
(17) \quad \sigma_R(R,\theta) = \sum_{n=1}^{9} \beta S_n \left\{ \frac{n}{4} R^{\frac{n}{2}-1} \left[-(n+2)\cos(\tfrac{n}{2}+1)\theta + f(n)(n-6)\cos(\tfrac{n}{2}-1)\theta \right] \right\}
$$

$$
+ \sum_{n=1,3}^{9} \beta A_n \left\{ \frac{n}{4} R^{\frac{n}{2}-1} \left[g(n)(n+1)\sin(\tfrac{n}{2}+1)\theta - (n-6)\sin(\tfrac{n}{2}-1)\theta \right] \right\}
$$

$$
(18) \quad \sigma_\theta(R,\theta) = \sum_{n=1}^{9} \beta S_n \left\{ \frac{n}{4} R^{\frac{n}{2}-1} \left[(n+2)\cos(\tfrac{n}{2}+1)\theta - f(n)\cos(\tfrac{n}{2}-1)\theta(n+2) \right] \right\}
$$

$$
+ \sum_{n=1,3}^{9} \beta A_n \left\{ \frac{n}{4} R^{\frac{n}{2}-1} \left[-g(n)(n+2)\sin(\tfrac{n}{2}+1)\theta + (n+2)\sin(\tfrac{n}{2}-1)\theta \right] \right\}
$$

and

$$
(19) \quad \tau_{R\theta}(R,\theta) = \sum_{n=1}^{9} \beta S_n \left\{ \frac{n}{4} R^{\frac{n}{2}-1} \left[(n+2)\sin(\tfrac{n}{2}+1)\theta - f(n)(n-2)\sin(\tfrac{n}{2}-1)\theta \right] \right\}
$$

$$
+ \sum_{n=1,3}^{9} \beta A_n \left\{ \frac{n}{4} R^{\frac{n}{2}-1} \left[g(n)(n+2)\cos(\tfrac{n}{2}+1)\theta - (n-2)\cos(\tfrac{n}{2}-1)\theta \right] \right\}
$$

in which

$$
f(n) = \frac{\frac{n}{2}+1}{\frac{n}{2}+(-1)^n}
$$

and

$$
g(n) = \frac{\frac{n}{2}-(-1)^n}{\frac{n}{2}+1}
$$

where βS_n and βA_n are the symmetric and antisymmetric parts of $\{\beta\}$.

186

The symmetric and antisymmetric coefficients βS_1 and βA_1 are associated with the singularity $R^{-1/2}$. They are related to the opening and sliding mode stress intensity factors K_1 and K_{11} by the following formulas

(20) $K_1 = 3 \sqrt{2\pi} \, \beta S_1$

(21) $K_{11} = \sqrt{2\pi} \, \beta A_1$

Hence once the displacements $\{ Q \}$ have been determined the leading coefficients βA_1 and βS_1 can be recovered through (15) and subsequently the stress intensity factors through (20) and (21).

IMPLEMENTING THE CRACK ELEMENT INTO NASTRAN

The nine node crack element has been implemented into NASTRAN through the dummy element capability. This capability permits a user to enter his own element subroutines for the purpose of generating the stiffness and mass matrix contributions, the thermal load contributions and for the computation of various stresses and forces for output (see section 8.8.5 of the NASTRAN PROGRAMMERS MANUAL, Reference 3). This procedure is relatively simple compared to adding an entirely new element to the system.

The crack element has been implemented as a DUM2 element. The format for the ADUM2, CDUM2, and PDUM2 bulk data cards which are used to enter the geometry, property, and connectivity data is shown in Figure 2. The procedure used to implement the element is as follows.

o   Create an element stiffness subroutine KDUM2 which computes and outputs to functional module SMA1 one 6 x 6 matrix for each connecting grid point with respect to the connective pivot point.

o   Create two subroutines SDUM21 and SDUM22 to compute and output to functional module SDR2 the stress intensity factors.

o   Remap LINK3 to include the new routine KDUM2 and LINK13 to include the new routines SDUM21 and SDUM22.

All the element stiffness subroutines called by SMA1, including KDUM2, are overlayed.   Therefore to avoid reducing the working core available to SMA1, KDUM2 was programmed in less core than the largest amount used by any of the existing element stiffness routines.   To do this it was necessary to fix the shape of the element shown in Figure 1.   Chosen was a square with the nine grid points equally spaced around the boundary.   This made it possible to compute the integrations involved in (13) and (14) externally to NASTRAN for a unit element size.   Further (13) was integrated for a unit value of each of the two independent coefficients for an isotropic material in the compliance matrix $\begin{bmatrix} S \end{bmatrix}$ i.e.

$$\begin{bmatrix} S \end{bmatrix} = S_1 \begin{bmatrix} 1 & 0 & 0 \\ 0 & 1 & 0 \\ 0 & 0 & 2 \end{bmatrix} + S_2 \begin{bmatrix} 1 & 1 & 0 \\ 1 & 1 & 0 \\ 0 & 0 & 0 \end{bmatrix}$$

where

$$S_1 = 1/2G$$

$$S_2 = \begin{cases} -v/2G & \text{PLANE STRAIN} \\ -v/2G(1+v) & \text{PLANE STRESS} \end{cases}$$

The resulting unit matrix for $\begin{bmatrix} KA \end{bmatrix}$ and the two unit matrices for $\begin{bmatrix} KC \end{bmatrix}$ are used as permanent data in the subroutines KDUM2 and SDUM21.

Subroutine KDUM2 forms the matrices $\begin{bmatrix} KA \end{bmatrix}$ and $\begin{bmatrix} KC \end{bmatrix}$ in double precision from the three unit matrices for a specific element size and material.   It then uses these in (16) to compute the 2 x 2 stiffness matrices in the local element coordinate system for each grid point associated with the respective connective pivot point. Finally it transforms these 2 x 2 matrices into 6 x 6 matrices in the global coordinate system.

Similarly subroutine SDUM21 forms the matrices $\begin{bmatrix} \mathbf{KA} \end{bmatrix}$ and $\begin{bmatrix} \mathbf{KC} \end{bmatrix}$ in single precision for a specific element size and material. It then computes the two stress intensity factors $\mathbf{K}_1$ and $\mathbf{K}_{11}$ for a unit value of each of the grid point displacements $\{ \mathbf{Q} \}$ in the global system using 15, 20, and 21. Subroutine SDUM22 computes the final stress intensity factors for specific grid point displacements.

ELEMENT EVALUATION

The capability of the element to predict accurate stress intensity factors has been demonstrated by numerous analyses. Two are presented here for which there are known classic solutions.

The opening mode stress intensity factor for an isotropic material can be expressed in the form, Reference 4.

(22) $\mathbf{K}_1 = \sigma \sqrt{\pi a} \ f$

Where $\sigma \sqrt{\pi a}$ is the stress intensity factor for a central crack of length 2a in an infinite plate loaded by a far field stress σ acting normal to the crack. f is either the correction factor associated with Bowie's analysis for the presence of a hole, Reference 5, or Isida's analysis for a finite width plate, Reference 6.

The finite element model shown in Figure 3 represents a crack in a finite width plate loaded by a far field stress acting normal to the crack. The plate is 81 cm wide 168 cm long and the crack length is varied between 10 and 51 cm. The model which idealizes one quarter of the plate represents the full structure thru the use of symmetric boundary constraints. The crack element which overlaps a symmetry boundary is forced to deflect symmetrically thru the use of multi-point constraint equations. It should be noted that when the multipoint constraint equations are used in this way the element that is being forced to act symmetrically should be specified with half its actual thickness. Besides the DUM2 crack element the model consists of 66 CQDMEM elements, and 36 CTRMEM elements. It has 124 grid points, 219 active freedoms, and a semiband width of 37. Figure 3 shows that for this type of idealization the crack element computes the stress intensity $\mathbf{K}_1$ to within 3% of that given by equation (22).

The finite element model shown in Figure 4 represents symmetric cracks protruding from a hole in the center of an infinite plate. The plate is 102 cm wide and 102 cm long. The hole has a diameter of 5 cm and the crack lengths are varied between 0.8 and 8 cm . The model uses the same idealization techniques employed in the previous example to represent the plate. It consists of 154 CQDMEM elements, 5 CTRMEM elements and one DUM2 crack element. Figure 4 shows the results to be within 3% of equation 22.

C5A FAILSAFE ANALYSIS

The C5A fuselage has a failsafe criterion which requires that a 30 cm longitudinal crack in the cover skin will not result in a catastrophic failure when the structure is subjected to a normal operating internal pressure. To satisfy this requirement, circumferential failsafe straps are attached to the skin mid way between the frames for the purpose of arresting such a crack, see Figure 5. An analysis based on Lockheed data sheets is conservative and as a result dictates the use of expensive high strength fasteners to attach the strap to the skin. The following analysis using NASTRAN shows that less expensive aluminum rivets can be used instead.

As a longitudinal skin crack passes under the failsafe strap the stress intensity at the tip reduces. The crack will cease to propagate if the stress intensity becomes less than the critical stress intensity for the material, provided that the fasteners in the strap do not fail first. The finite element model shown in Figure 6 represents a typical region of the C5A aft fuselage. It considers the frame at fuselage station (F.S.) 1804 to be failed and is used to analyze various lengths of a skin crack which propagates towards the failsafe straps at F.S.'s 1794 and 1814. The model is two-dimensional, i.e. fuselage curvature and out of plane deflections are ignored. Advantage has been taken of two symmetry planes by idealizing only one quarter of the actual damaged region. The crack element which lies across a symmetry boundary is again forced to displace symmetrically through the use of multi-point constraint equations. The frame cap and the skin are represented as an integral structure through the use of CROD,CTRMEM, CQUAD, and the CDUM2 elements. The strap which is considered as a separate unit uses the CTRMEM and CQUAD elements. The twelve fasteners closest to the crack are each idealized by a system of CROD elements. The remaining fasteners are lumped into groups of approximately 4 and idealized by CELASI elements. The model is loaded by concentrated forces which represent the hoop loading on a 244 cm radius structure for a normal operating internal pressure with a dynamic factor of 1.15. The loading is applied to the model in proportion to the circumferential cross sectional area. This does not represent the true circumferential loading as it neglects the bulging effect of the skin between the frames. It is conservative however in that it overloads the frame at the center of the crack.

In order to show the fasteners capable of carrying the transfer load it is necessary to consider the nonlinear load deflection response for the twelve fasteners closest to the crack, see figure 7. Because the CELASI elements do not have the capability of representing nonlinearity it was necessary to idealize these fasteners by the system of CROD elements shown in Figure 8. The rods connect the coincidental grid points A and B on the skin and strap respectively through the grid point C. The elements have a combined length of 2.54 cm (1 in.) and a cross-sectional area of 6.45 cm^2 (1 in^2). The use of English units allows the load deflection curves in Figure 7 to be input directly on Tables 1 cards as a stress strain curve for the rod elements. The only other region of the structure to experience plasticity is the tip of the crack and since this is ignored in linear fracture mechanics the most economical way of executing the analysis is to divide the model into two substructures: the skin, frame, and strap being included in substructure 1 and the fasteners in substructure 2. Substructure 1 is analyzed first for an increment of the external loads using rigid format 1. The freedoms for the grid points common to the fasteners are included in the 'A' set and the rigid format altered to terminate once the reduced A set stiffness and loads matrices are formed. Substructure 2 is then analyzed using rigid format 6, the piecewise linear analysis. Rigid format 6 is altered to read the A set stiffness and loads matrices for substructure 1 and add them to the appropriate terms in the G set stiffness and loads matrices for substructure 2. The results of the piecewise linear analysis give the desired fastener loads. To obtain the stress intensity factor it is necessary to restart the analysis for substructure 1 using the A set displacements resulting from the analysis of substructure 2.

Substructure 1 consists of one CDUM2, 56 CROD, 71 CTRMEM and 814 CQDMEM elements. It has 952 grid points, 1876 active freedoms and a semiband width of 84. There are 136 freedoms in the A set for which it took 31 CPU minutes, on a UNIVAC 1106 computer executed in a time sharing mode, to form the reduced stiffness and loads matrices. Substructure 2 consists of 56 CELASI elements and 24 CROD elements. It has 80 grid points, 148 active freedoms and a semiband width of 142. It took 10 iterations to obtain the elastic-plastic solution using 14 CPU minutes. The back feed into substructure 1 to obtain the stress intensity factor ran for 8 CPU minutes. All the above run times are for Level 15.1.

The analysis has been made for both the original 3.2 mm (1/8 in.) YBO TAPERLOKS and the proposed 4.0 mm (5/32 in.) aluminum rivets. Four crack lengths were considered for each system, the results being plotted in Figures 9 and 10 respectively. They show the ratio of the stress intensity to the critical stress intensity (K_1/K_c) and the ratio of the maximum fastener load to the allowable fastener load (P/P_a) plotted against the half crack length. Figure 9 shows that when the TAPERLOKS are used the stress intensity reduces to the critical value at a half crack length of 22 cm. At this length the fasteners are only working to 40% of their allowable load; hence they are shown to provide the necessary failsafe characteristics. This is only to be expected as the more conservative Lockheed data sheets also show the TAPERLOKS capable of arresting the crack. Figure 10 shows that when the rivets are used the stress intensity reduces to the critical value at a half crack length of 24 cm. At this length

the rivets are working to 67% of their allowable load therefore, unlike the conventional analysis, this analysis shows that they also are capable of providing the necessary failsafe characteristics. This analysis was validated by a test program which demonstrated that the rivets are capable of arresting the skin crack.

CONCLUSION

The NASTRAN capability of allowing a user to implement a dummy element was found to be relatively simple to use and exceedingly useful.   Lockheed Georgia Company has plans to implement more elements into the system.   In particular work is underway on a fastener element, similar to CELAS1, that has the capability of representing a nonlinear load deflection curve.

REFERENCES

1.   Fung, Y.C.: Foundations of Solid Mechanics.   Prentice-Hall Inc., 1965, pg 300.

2.   Aberson, J.A., Anderson, J.M.: Cracked Finite Elements Proposed for NASTRAN. NASTRAN: User's Experiences.   NASA TM X-2893, 1973

3.   The NASTRAN Programmer's Manual.   NAS SP-223 (01), Sept. 1972.

4.   Bowie, O. L.: Analysis of an Infinite Plate Containing Radial Cracks Originating from the Boundary of an Internal Circular Hole.   Journal of Mathematics on Physics, Vol. 35, 1956.

5.   Isida, M.: On the Tension of a Strip with a Central Elliptical Hole. Transactions, Japanese Society of Mechanical Engineers, Vol. 22, 1956.

6.   Wilhem, D.P.: Fracture Mechanics Guidelines for Aircraft Structural Application. AFFDL-TR-69-111, February 1970.
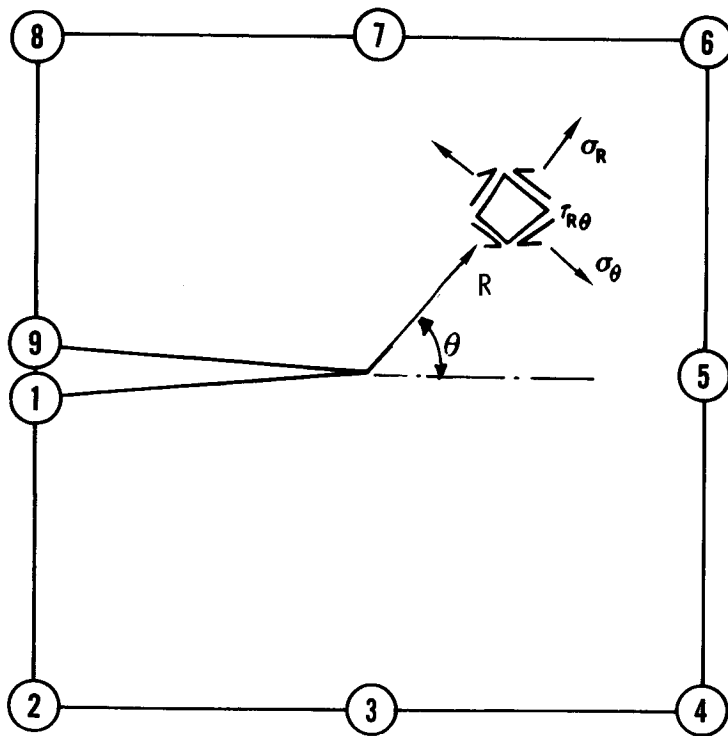
Figure 1. Nine Node Crack Element

ADUMi	NG	NC	NP	ND					
ADUM2	9	0	2	3					

CDUM2	EID	PID	G1	G2	G3	G4	G5	G6	abc
CDUM2	1	1	1	2	3	4	5	6	abc

+bc	G7	G8	G9					
+bc	7	8	9					

PDUM2	PID	MID	t	N				
PDUM2	1	1	.5	1				

WHERE

NG   NUMBER OF GRID POINTS CONNECTED BY DUM2 CRACK ELEMENT
NC   NUMBER OF ADDITIONAL ENTRIES ON CDUM2 CONNECTION CARD
NP   NUMBER OF ADDITIONAL ENTRIES ON PDUM2 PROPERTY CARD
ND   NUMBER OF DISPLACEMENT COMPONENTS AT EACH GRID POINT
EID   ELEMENT IDENTIFICATION NUMBER
PID   IDENTIFICATION NUMBER OF A PDUM2 PROPERTY CARD
Gi   GRID POINT IDENTIFICATION NUMBERS OF CONNECTION POINTS
MID   MATERIAL IDENTIFICATION NUMBER
t   ELEMENT THICKNESS
N   N=1 INDICATES PLANE STRESS
      N=0 INDICATES PLANE STRAIN

Figure 2.   Bulk Data Cards For a DUM2 Crack Element
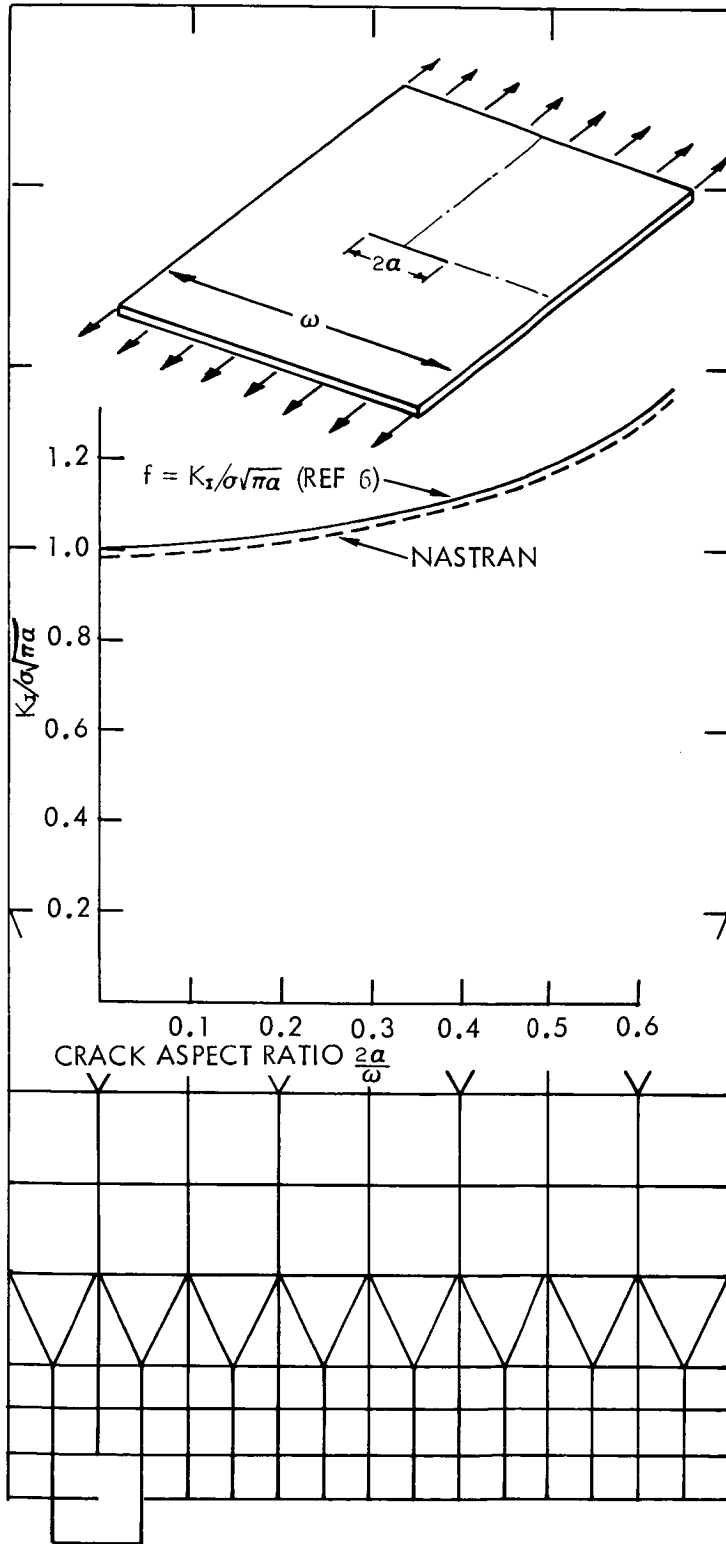
Figure 3. K_1 Comparison For a Central Crack in a Finite Width Plate.
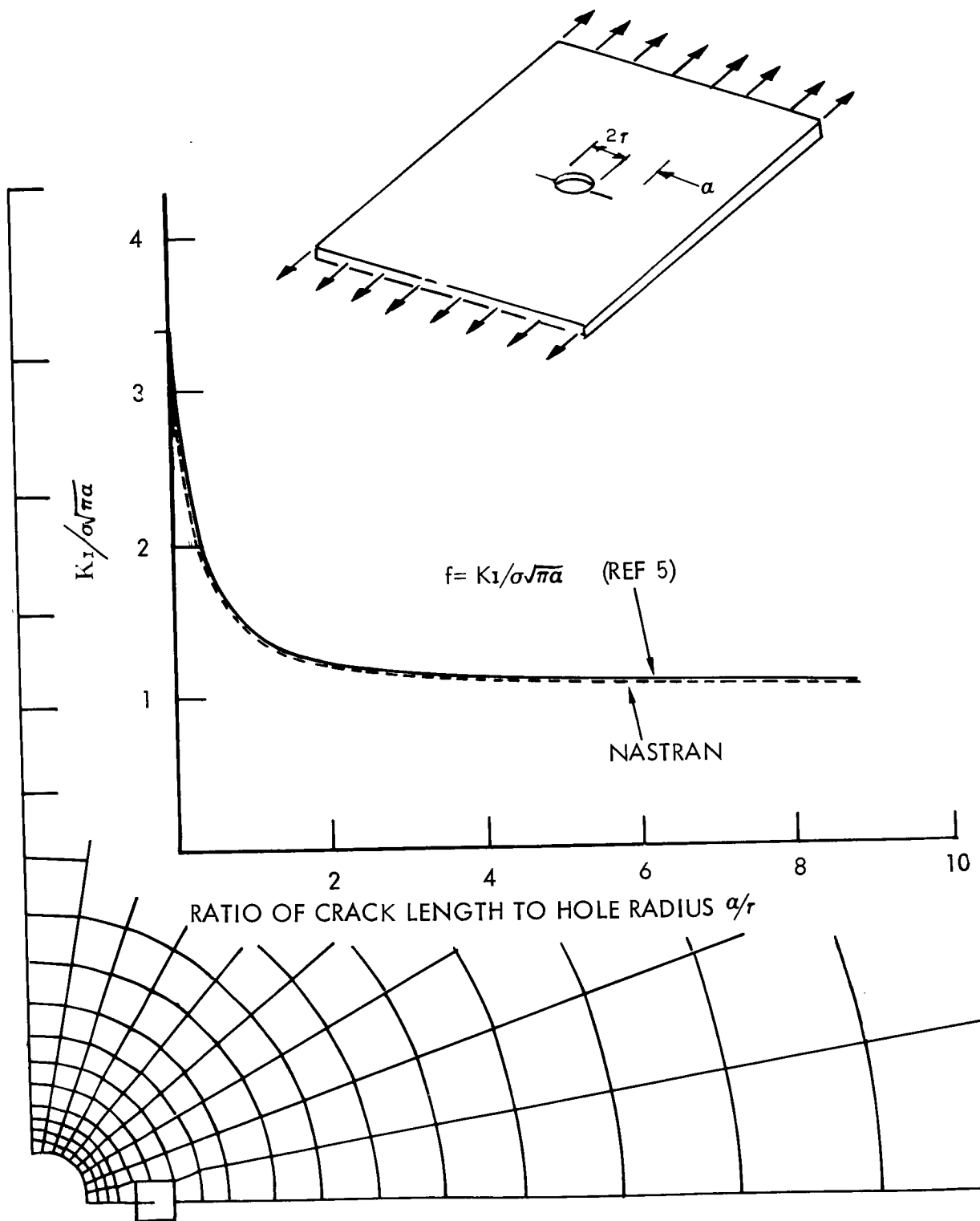
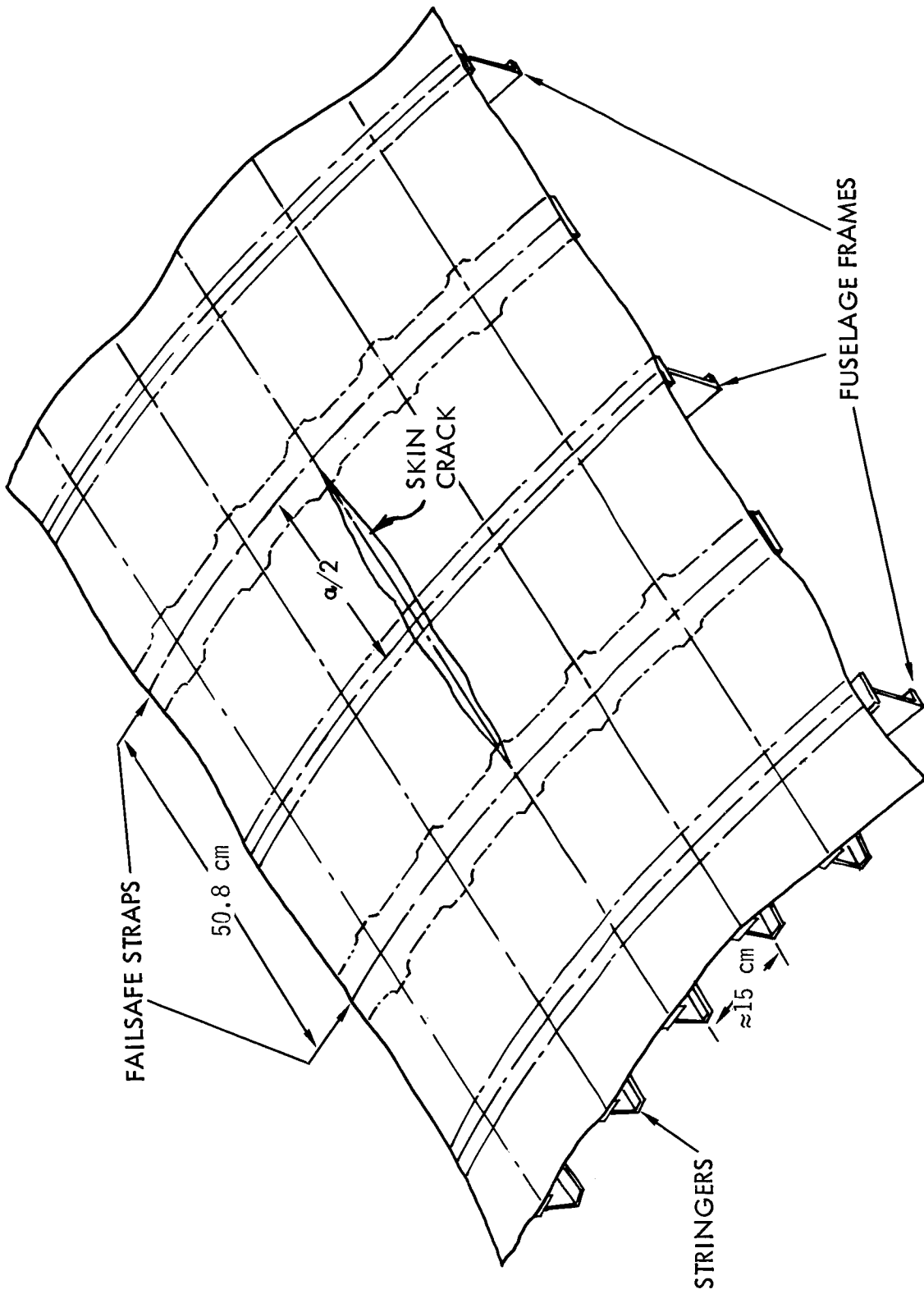Figure 4. K_I Comparison For Symmetric Cracks at a Hole in an Infinite Plate

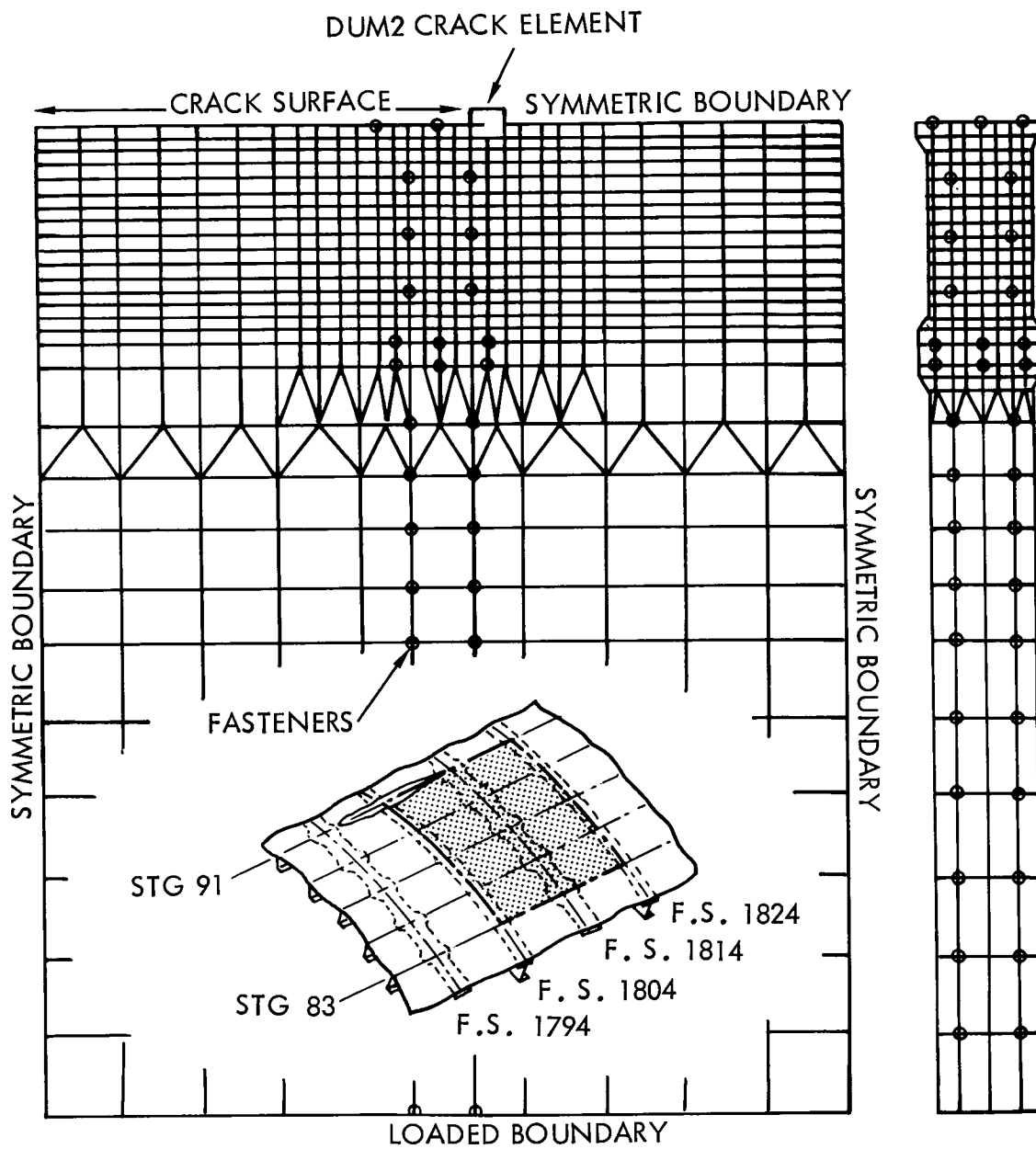Figure 5. C5A Cracked Skin Configuration.

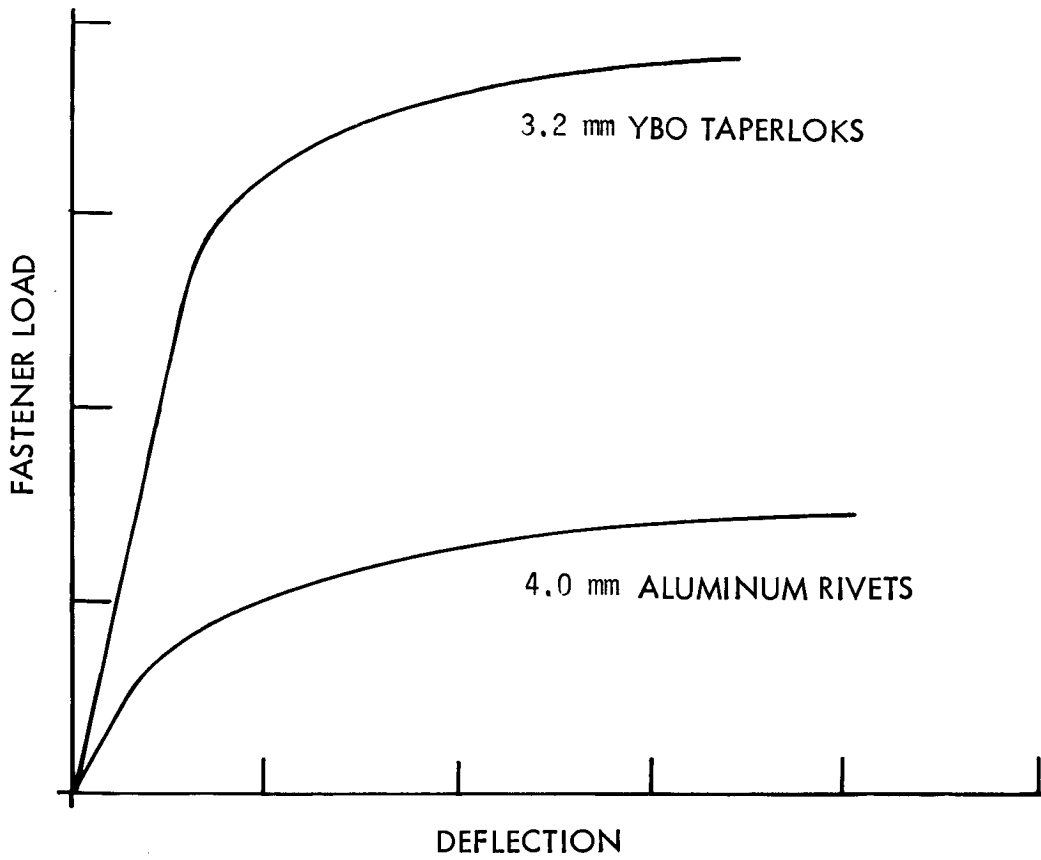Figure 6. NASTRAN Model of a C5A Fuselage Skin Crack

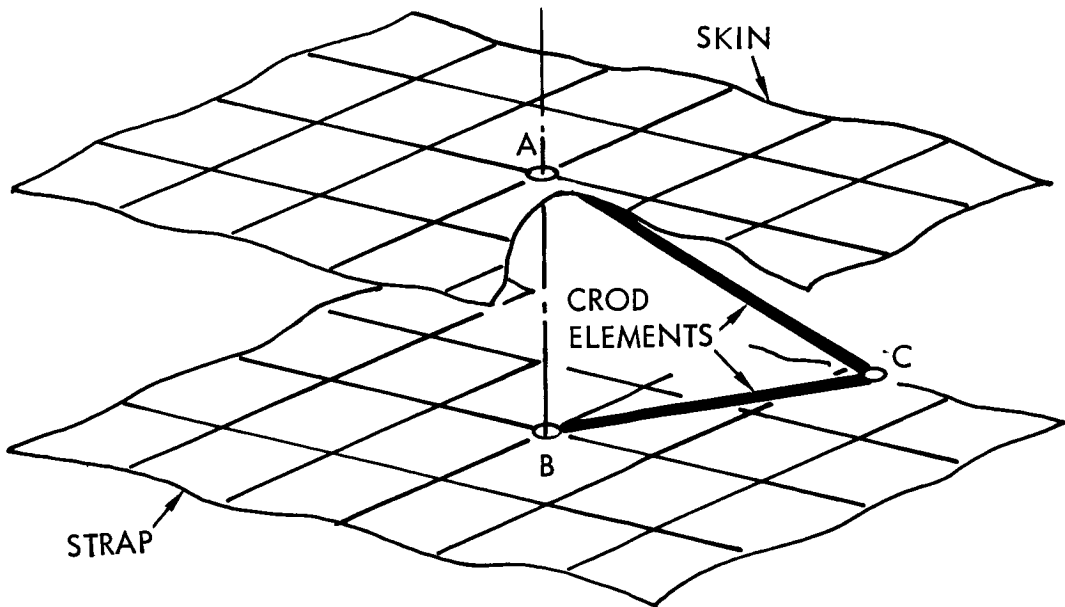Figure 7. Nonlinear Fastener Load-Deflection Curves
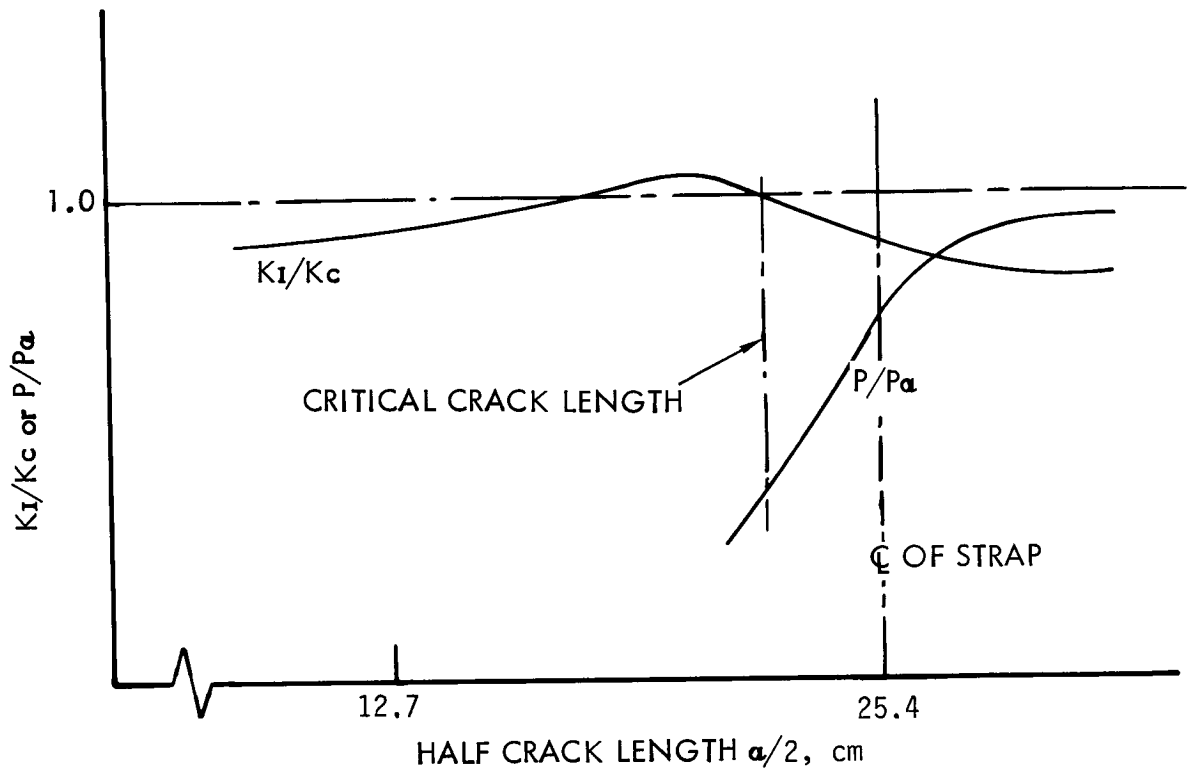

Figure 8. Fastener Idealization

Figure 9. NASTRAN Results From the Finite Element Model
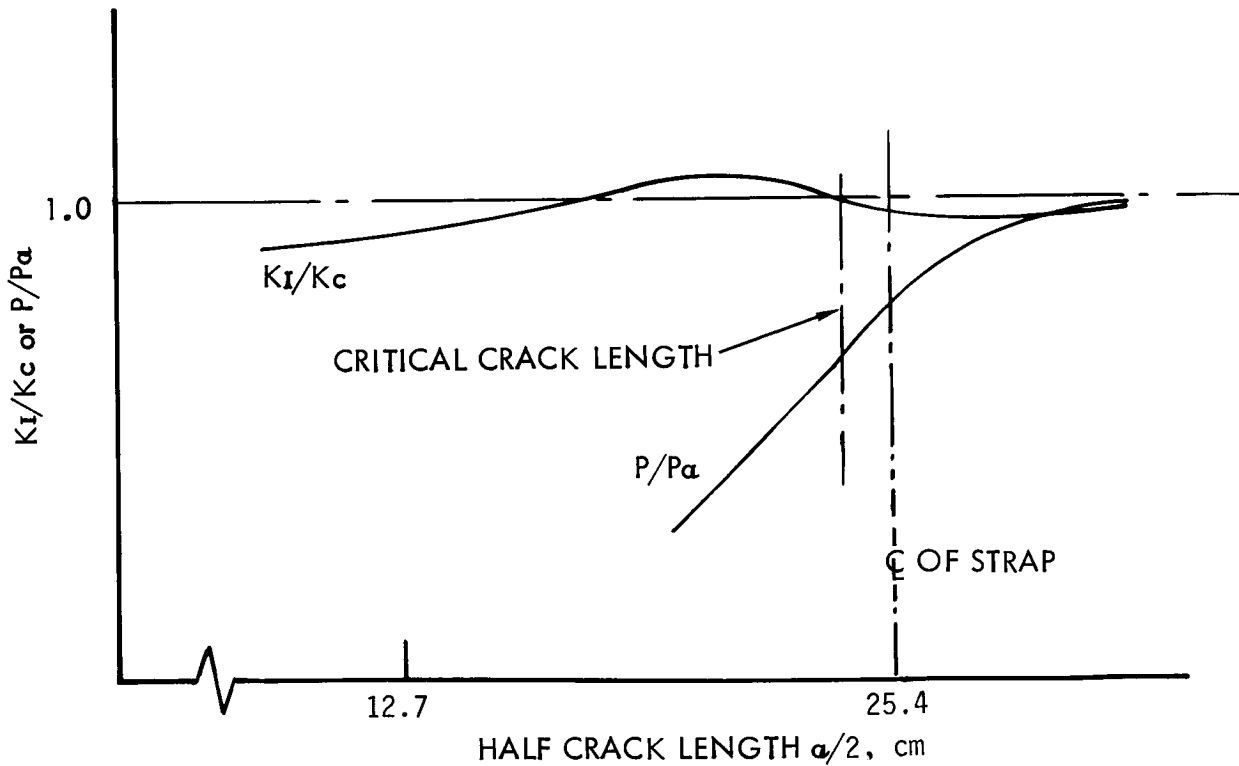Shown in Figure 6 for 3.2 mm TAPERLOKS.

Figure 10. NASTRAN Results From the Finite Element Model
Shown in Figure 6 for 4.0 mm Aluminum Rivets.